Acta Crystallographica Section E
Structure Reports Online
ISSN 1600-5368

A nitrobenzene and dimethylformamide clathrate of (pyridine)[5,10,15-tris(4-cyanophenyl)-20-(2-quinolyl)porphyrinato]zinc(II)

Sankar Muniappan, Sophia Liptsman and Israel Goldberg*

School of Chemistry, Sackler Faculty of Exact Sciences, Tel-Aviv University, Ramat-Aviv, 69978 Tel-Aviv, Israel

Correspondence e-mail: goldberg@post.tau.ac.il

Key indicators

Single-crystal X-ray study
T = 110 K
Mean σ(C–C) = 0.004 Å
R factor = 0.056
wR factor = 0.154
Data-to-parameter ratio = 19.2

For details of how these key indicators were automatically derived from the article, see http://journals.iucr.org/e.

Received 1 March 2006
Accepted 5 March 2006

The title compound, $[Zn(C_{50}H_{26}N_8)(C_5H_5N)]\cdot C_6H_5NO_2\cdot C_3H_7NO$, is a nitrobenzene clathrate of a five-coordinate zinc–pyridine–porphyrin complex with different substituents at the *meso* positions of the metalloporphyrin core. The complex adopts a domed conformation with the central zinc ion deviating from the plane of the macrocyclic ring towards the apical pyridine ligand. The crystal packing is characterized by a layered arrangement of the porphyrin molecules with dipole–dipole interactions and weak hydrogen bonding contributing to the stabilization of the crystal structure. While the nitrobenzene solvent is well localized within the open porphyrin layers, molecules of the dimethylformamide are severely disordered in elongated interlayer channel voids

Comment

The porphyrin ligand of the title compound, (I) (Fig. 1), is a precursor to asymmetrically functionalized porphyrin building blocks [*e.g.* tris(hydroxyphenyl)(quinolyl)porphyrin] used by us in the supramolecular synthesis of porphyrin-based network solids with increased odds of exhibiting non-centrosymmetric architectures (Goldberg, 2005; Vinodu & Goldberg, 2003; Vinodu & Goldberg, 2005). Here, (I) crystallized as a nitrobenzene and dimethylformamide clathrate, molecules of the former being intercalated between aromatic fragments of the porphyrin host. The geometry of the metalloporphyrin is normal (Table 1).

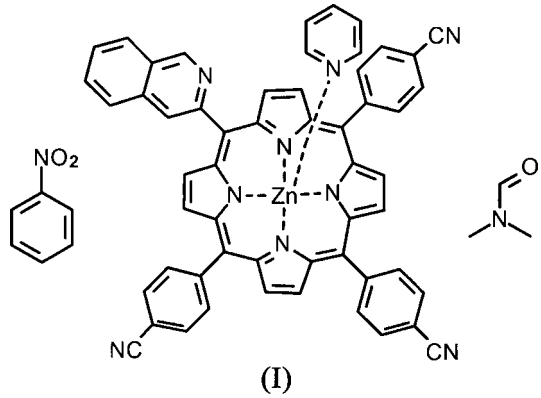

(I)

As commonly observed in five-coordinate complexes of zinc–metalloporphyrins, the central zinc ion deviates by 0.372 (1) Å from the mean plane of the four coordinating pyrrole N atoms towards the apical N atom (Byrn *et al.*, 1993; Lipstman & Goldberg, 2006; Lipstman *et al.*, 2006; Allen, 2002). Correspondingly, the macrocyclic core of the porphyrin unit is slighly distorted from planarity (Fig. 2). This distortion is reflected by the dihedral angles between the

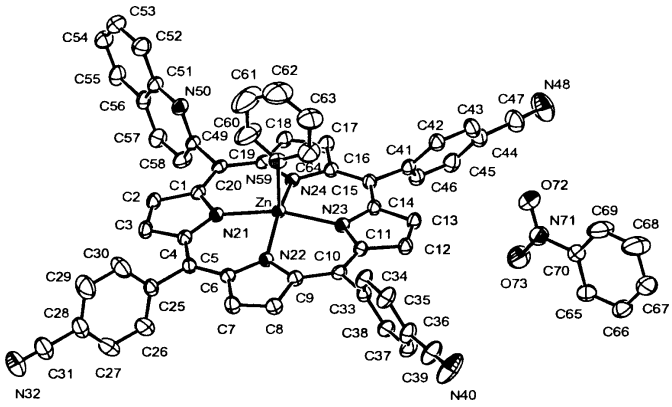

Figure 1
The molecular structure of (I), showing 40% probability displacement ellipsoids. H atoms have been omitted for clarity.

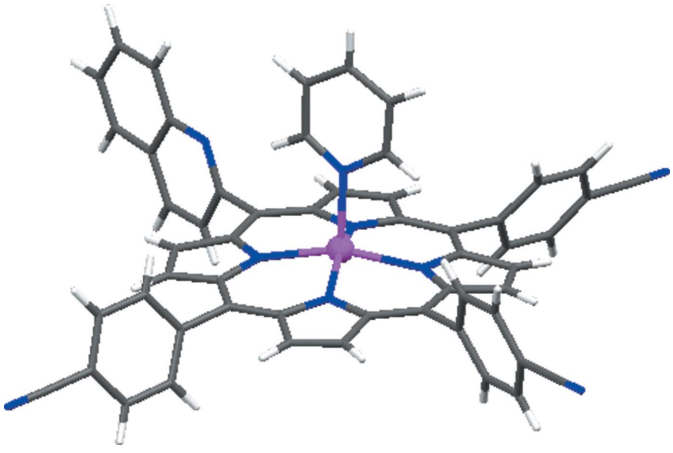

Figure 2
Perspective view of the domed molecular structure of the five-coordinate zinc–pyridine–porphyrin complex in (I). The nitrobenzene solvent has been excluded. Color code: Zn pink, N blue, C dark gray and H white.

N_4-pyrrole plane and the planes of the individual pyrrole rings. These angles are 7.98 (14), 5.31 (15), 3.66 (14) and 5.51 (14)° for the pyrrole rings containing atoms N21, N22, N23 and N24, respectively, all of which tilt away from the apical ligand. The metalloporphyrin species arrange in the form of open layers, which are sustained by dipole–dipole interactions between antiparallel (inversion-related) cyanophenyl fragments of adjacent units as well as by weak C—H(pyrrole)···NC hydrogen bonds (Fig. 3 and Table 2).

The four aryl arms of a given porphyrin unit are essentially in a 'stacking' contact with the corresponding aryl groups of the surrounding units. For the two pairs of overlapping cyanophenyl residues and the two pairs of cyanophenyl–quinolyl groups, the individual atoms of one component are positioned within the 3.2–3.9 Å range above the mean plane of the other component. The observed network is similar to that found previously in the crystal structures of tetrakis(4-cyanophenyl)porphyrins (Krishna Kumar *et al.*, 1998). Adjacent inversion-related layers fit well into one another; the apical pyridine ligands of one layer are inserted within the interporphyrin voids of the other layer in a lock-and-key

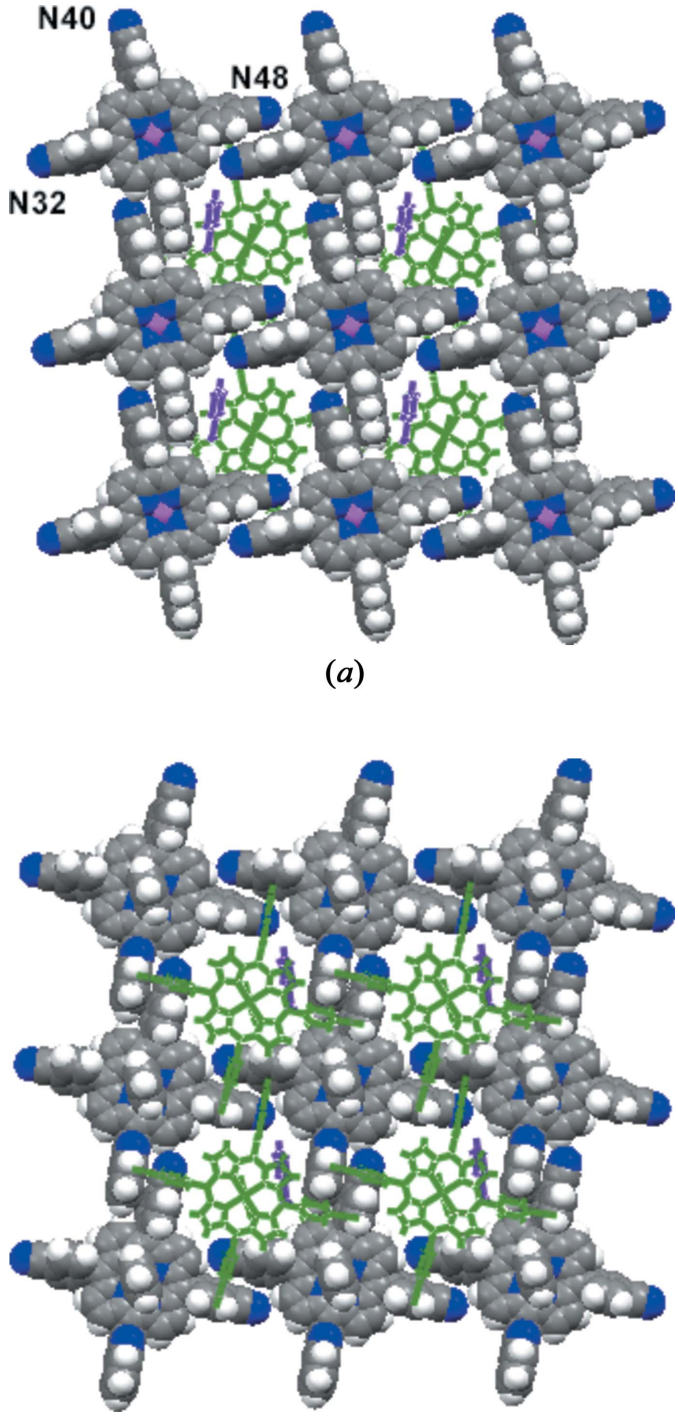

Figure 3
Space-filling illustration of the interporphyrin organization as an open layer in (I), showing also in stick representation an adjacent inversion-related porphyrin layer (in green) and the nitrobenzene solvent (in violet). Note the lock-and-key-type fit between the two layers. Molecules along the horizontal direction of this figure are displaced along the *a*–*b* axis of the crystal, while those along the nearly vertical direction are displaced along the *c* axis of the crystal. The concave and the domed surfaces of the space-filling layer are shown in (*a*) and (*b*), respectively. Color code for the space-filling layer: Zn pink, N blue, C dark gray and H white.

mode. As the pyridine ligand is too small to fill these voids effectively by itself, nitrobenzene molecules from the crystallization solvent are incorporated edge-on into the voids as well. At any given site, the aromatic rings of the pyridine and nitrobenzene groups are roughly parallel to one another. Thus, the formed porphyrin bilayers stack back-to-back one on top of the other in an offset manner, the nitrobenzene molecules located on the surfaces of one bilayer being placed just opposite, and filling the space on, the concave faces of the dome-shaped metalloporphyrin units of neighboring bilayers on both sides (Fig. 4). Such an effective fit between the layered porphyrin–nitrobenzene domains allows for their tight stacking in the crystal structure. The latter is also reflected in weak C—H···O and C—H···N interactions between molecules located in inversion-related layers (Table 2). Still, channel voids are present in the crystal lattice between the porphyrin layers around $(x,\frac{1}{2},\frac{1}{2})$ (Fig. 4). They appear to be accommodated by severely disordered dimethyformamide solvent, which could not be modeled reliably with discrete atoms (see *Experimental*).

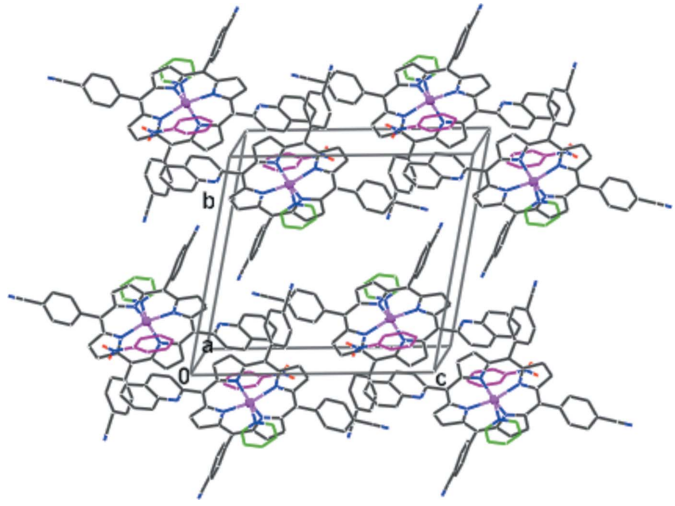

Figure 4
Perspective view of the crystal structure, approximately down the *a* axis. The carbon framework of the porphyrin is shown in black, that of the nitrobenzene solvent in violet, and that of the pyridine axial ligand in green. Otherwise, the N and O atoms are marked in blue and red, respectively. Note the small intermolecular void centered at $(x, \frac{1}{2}, \frac{1}{2})$, in which the severely disordered dimethylformamide solvent is accommodated.

Experimental

The synthetic methodology of the condensation of pyrrole, 4-cyanobenzaldehyde and 2-quinolinecarbaldehyde, resolving the mixture of products on a column, and reacting the desired isomer with zinc acetate, was reported earlier (Vinodu & Goldberg, 2003; Vinodu & Goldberg, 2005), following known literature procedures by Adler *et al.* (1967) and Rao *et al.* (2000). Red single crystals of (I) were obtained by dissolving about 2.5 mg of the zinc–porphyrin in a mixture of pyridine and dimethylformamide (5 ml) and a few drops of nitrobenzene, followed by slow crystallization under ambient conditions.

Crystal data

$[Zn(C_{50}H_{26}N_8)(C_5H_5N)]\cdot C_6H_5NO_2\cdot C_3H_7NO$	$Z = 2$
$M_r = 1079.46$	$D_x = 1.305$ Mg m^{-3}
Triclinic, $P\overline{1}$	Mo $K\alpha$ radiation
$a = 11.2089$ (2) Å	Cell parameters from 10058 reflections
$b = 15.3117$ (3) Å	$\theta = 1.4$–$27.9°$
$c = 17.2043$ (4) Å	$\mu = 0.51$ mm^{-1}
$\alpha = 79.6017$ (12)°	$T = 110$ (2) K
$\beta = 72.0928$ (11)°	Needle, red
$\gamma = 80.9992$ (16)°	0.35 × 0.15 × 0.10 mm
$V = 2747.42$ (10) Å^3	

Data collection

Nonius KappaCCD diffractometer	$R_{int} = 0.044$
ω scans	$\theta_{max} = 27.9°$
Absorption correction: none	$h = -14 \rightarrow 14$
30139 measured reflections	$k = -19 \rightarrow 20$
12778 independent reflections	$l = -20 \rightarrow 22$
9650 reflections with $I > 2\sigma(I)$	

Refinement

Refinement on F^2	$w = 1/[\sigma^2(F_o^2) + (0.0847P)^2 + 0.5255P]$ where $P = (F_o^2 + 2F_c^2)/3$
$R[F^2 > 2\sigma(F^2)] = 0.056$	$(\Delta/\sigma)_{max} = 0.002$
$wR(F^2) = 0.154$	$\Delta\rho_{max} = 0.94$ e Å^{-3}
$S = 1.07$	$\Delta\rho_{min} = -0.47$ e Å^{-3}
12778 reflections	
667 parameters	
H-atom parameters constrained	

Table 1
Selected bond lengths (Å).

Zn—N21	2.0704 (19)	Zn—N23	2.0819 (19)
Zn—N22	2.0784 (19)	Zn—N59	2.129 (2)
Zn—N24	2.081 (2)		

Table 2
Hydrogen-bond geometry (Å, °).

D—H···A	D—H	H···A	D···A	D—H···A
C2—H2···N40^{a,i}	0.95	2.58	3.439 (4)	151
C7—H7···N48^{b,ii}	0.95	2.59	3.498 (4)	161
C38—H38···O73^{c,iii}	0.95	2.47	3.263 (4)	140
C58—H58···N24^{d,iv}	0.95	2.59	3.348 (3)	137
C68—H68···N50^{e,v}	0.95	2.57	3.482 (5)	162
C17—H17···N32^{f,vi}	0.95	2.96	3.828 (4)	153

Symmetry codes: (i) $x, y, z-1$; (ii) $x+1, y-1, z$; (iii) $-x+1, -y+1, -z+1$; (iv) $-x+1, -y+2, -z$; (v) $-x, -y+1, -z+1$; (vi) $x-1, y+1, z$.

The H atoms were placed in calculated positions and were constrained to ride on their parent atoms, with C—H = 0.95–0.98 Å and U_{iso}(H) = 1.2U_{eq}(C) or 1.5U_{eq}(C). Results of the least-squares refinement calculations suggest that the axial pyridine ligand as well as the nitrobenzene solvent are partly disordered in their orientation, as the displacement parameters of some C atoms in these rings are markedly elongated perpendicular to the corresponding ring (Fig. 1). This apparent disorder could not be reliably resolved. Moreover, in addition to the nitrobenzene, (I) was found to contain also some amount of severely disordered dimethylformamide solvent trapped in the lattice in voids centered at the $(0, \frac{1}{2}, \frac{1}{2})$ inversion center and elongated along the *a* axis of the crystal structure (Fig. 4). Conventional refinement converged at $R = 0.086$, showing recognizeable

fragments of at least two dimethylformamide solvent species with partial occupancies, but rather high displacement parameters for the corresponding atoms, and distorted geometries. Still, 3–4 residual electron-density peaks within 1.5–2.0 e Å^{-3} could not be accounted for. Correspondingly, it was preferred to subtract the contribution of the dimethylformamide solvent from the diffraction data by the SQUEEZE procedure in *PLATON* (Spek, 2003). The modified calculations converged smoothly at a considerably lower *R* factor. The solvent-accessible void centered at (0, $\frac{1}{2}$, $\frac{1}{2}$) was estimated to be 468 Å^3, about 17% of the unit-cell volume. The residual electron-density count was assessed as 86 electrons per unit cell, which is consistent with approximately two molecules of dimethylformamide.

Data collection: *COLLECT* (Nonius, 1999); cell refinement: *DENZO* (Otwinowski and Minor, 1997); data reduction: *DENZO* (Otwinowski and Minor, 1997); program(s) used to solve structure: *SIR97* (Altomare *et al.*, 1994); program(s) used to refine structure: *SHELXL97* (Sheldrick, 1997); molecular graphics: *ORTEP*-III (Burnett and Johnson, 1996) and *MERCURY* (Bruno *et al.*, 2002); software used to prepare material for publication: *SHELXL97* (Sheldrick, 1997).

This research was supported in part by The Israel Science Foundation (grant No. 254/04).

References

Adler, A. D., Longo, F. R., Finarelli, J. D., Goldmacher, J., Assour, J. & Korsakoff, L. (1967). *J. Org. Chem.* **32**, 476.

Allen, F. H. (2002). *Acta Cryst.* B**58**, 380–388.

Altomare, A., Burla, M. C., Camalli, M., Cascarano, M., Giacovazzo, C., Guagliardi, A. & Polidori, G. (1994). *J. Appl. Cryst.* **27**, 435.

Bruno, I. J., Cole, J. C., Edgington, P. R., Kessler, M., Macrae, C. F., McCabe, P., Pearson, J. & Taylor, R. (2002). *Acta Cryst.* B**58**, 389–397.

Burnett, M. N. & Johnson, C. K. (1996). *ORTEPIII*. Report ORNL-6895. Oak Ridge National Laboratory, Tennessee, USA.

Byrn, M. P., Curtis, C. J., Hsiou, Y., Khan, S. I., Sawin, P. A., Tendick, S. K., Terzis, A. & Strouse, C. E. (1993). *J. Am. Chem. Soc.* **115**, 9480–9497.

Goldberg, I. (2005). *Chem. Commun.* pp. 1243–1254.

Krishna Kumar, R., Balasubramanian, S. & Goldberg, I. (1998). *Inorg. Chem.* **37**, 541–552.

Lipstman, S., George, S. & Goldberg, I. (2006). *Acta Cryst.* E**62**, m417–m419.

Lipstman, S. & Goldberg, I. (2006). *Acta Cryst.* E**62**, m158–m160.

Nonius (1999). *COLLECT*. Nonius BV, Delft, The Netherlands.

Otwinowski, Z. & Minor, W. (1997). *Methods in Enzymology*, Vol. 276, *Macromolecular Crystallography*, Part A, edited by C. W. Carter Jr & R. M. Sweet, pp. 307–326. New York: Academic Press.

Rao, P. D., Dhanalekshmi, S., Litter, B. J. & Lindsey, J. S. (2000). *J. Org. Chem.* **65**, 7323–7344.

Sheldrick. G. M. (1997). *SHELXL97*. University of Göttingen, Germany.

Spek, A. L. (2003). *J. Appl. Cryst.* **36**, 7–13.

Vinodu, M. & Goldberg, I. (2003). *CrystEngComm*, **5**, 490–494.

Vinodu, M. & Goldberg, I. (2005). *CrystEngComm*, **7**, 133–138.